Renewables:
Wind, Water, and Solar

ORIGINAL RESEARCH ARTICLE

Open Access

Influence of operating conditions on solar energy utilization efficiency of flat plate solar collector

Shubo Xiao[1], Ying Zhang[2], Kuiming Xia[1,2] and Jibo Long[2*]

Abstract

For the last 20 years, solar collectors have been developing rapidly in the use of energy in buildings. Under experimental conditions, the solar energy utilization efficiency (SEUE) of flat plate solar collectors (FPSC) can reach more than 80%, but the engineering application of SEUE is low, and even the collector heating cannot meet the design requirements. In this paper, based on the existing thermal performance of FPSC, the influence of ambient meteorological parameters and hot water system operation parameters on SEUE is studied using experimental tests and analytical calculations. The results reflected that the collectors connected to the auxiliary heaters will affect SEUE, with series-connected systems having greater SEUE than parallel-connected systems. When the solar radiation intensity was low, the SEUE of parallel-connected systems was more likely to be negative. Under calculated conditions, when the water inlet temperature was 20, 30, 40, and 50 °C, the SEUE of the collector was 0%, and the corresponding solar radiation intensity was 113, 184, 225, and 328 W/m^2, respectively. Reducing the average water temperature of the collector can reduce the heat loss in the energy conversion process between the collector and the air and increase the SEUE. When the solar radiation intensity was 500 W/m^2, the collector inlet temperature decreases from 50 °C to 30 °C, and the SEUE increased from 20.9% to 38.5%. The research results can provide a parameter basis for the design of the FPSC system, especially the connection mode of collector and auxiliary heat device, and the design of system water temperature.

Keywords: Flat plate solar collector, Solar radiation intensity, Solar energy utilization efficiency, Total heat loss, Connection mode

Introduction

The traditional energy consumption structure dominated by fossil energy has caused environmental problems, such as climate warming (U.S. Department of Energy, 2012). Developing renewable energy utilization technology is an effective method to solve environmental problems such as climate warming and achieve the goal of carbon neutrality (Jonas et al., 2017; Wu et al., 2018). Solar energy has the advantages of no pollution, easy access, and low cost. It is the most potential renewable energy resource. At present, solar energy utilization technologies mainly include photovoltaic, photothermal, and photochemical (Liu et al., 2021). Among them, the application of photothermal technology has a long history and has been widely used in building heating systems, domestic hot water supplying systems, drying agricultural products, and so on (Zhang et al., 2017). The solar collector is a common solar energy utilization device (Tschopp et al., 2020). The solar hot water system is widely used to provide domestic and industrial hot water (Balaji et al., 2018), and a good solar hot water system can cater to 50–80% of users' needs for hot water (Ahmed et al., 2021). In

*Correspondence: longjibo2010@126.com

[2] College of Civil Engineering, Xiangtan University, Xiangtan 411105, Hunan, China
Full list of author information is available at the end of the article

recent years, solar hot water technology has been rapidly developed and widely applied (National energy., 2019). However, solar energy is intermittent with low energy density and easy to be affected by climate factors. This also leads to the low solar energy utilization efficiency (SEUE) of the collector. Therefore, how to improve the SEUE is still an important problem to be solved for the further popularization and application of photothermal technology (Jamar et al., 2016).

Generally, solar collectors include flat plate type, vacuum tube type, concentrating type and plane mirror, and so on (Gao et al., 2022). Among them, the flat plate solar collector (FPSC) has a simple structure and low cost, so it is widely used in the low-temperature solar system (Colangelo et al., 2016). However, the convective heat loss leads to a decrease in the SEUE of FPSC (Sokhansefat et al., 2018). To improve the SEUE, a great deal of research has been developed in improving the solar absorptance of the collector and reducing heat losses. In the structural design, the light transmittance of the collector is increased and the convective heat loss and radiation heat loss are reduced. Eaton proposed to create a vacuum environment to offset the convective heat transfer between FPSC and the external environment in 1975 (Eaton & Blu, 1975). After that, Gao et al. maintained the vacuum environment inside the collector by using glass–metal sealing technology and non-volatile getter. The average annual thermal efficiency can reach 50% for the collector (Gao et al., 2020). Ali et al. designed a vacuum FPSC with a curved cover and rear opaque insulation, which increased the available area of the absorber and cut the radiation heat transfer between the collector and the outside (Seddaoui et al., 2022). Johan et al. used inert gases with low thermal conductivity (such as AR and Kr) to fill the sealed space of the collector, which can reduce the thickness of the gas layer and heat loss by 20% (Vesthmd et al., 2009). Compared with ordinary FPSC, large-scale FPSC has a larger proportion of lighting area, smaller heat dissipation area, and higher thermal efficiency (Wang et al., 2022).

Increasing the solar energy absorption rate is another important method to improve the SEUE of the collector. The SEUE of the collector can be improved by increasing the transmittance of the glass cover plate and the solar absorptance of the heat-absorbing coating. After decades of development, the solar transmittance of the glass cover can reach 90% (Giovannetti et al., 2014). The solar heat-absorbing coating technology is relatively mature, and its solar absorptance is more than 90% (Qiu et al., 2021). In addition, adding IR mirror coating on the inner surface of the glass can reflect the thermal radiation emitted by the absorber plate, which can reduce the radiant heat loss (D'Alessandro et al., 2021). Joshi et al. developed antireflective coatings with an average solar transmittance of 98.1% (Joshi et al., 2019).

The collector temperature is another important factor affecting its heat loss. An increase in the thermal conductivity of the heat transfer fluid can lead to a decrease in the heat transfer temperature difference between the collector and the heat transfer fluid without reducing the heat transfer, to reduce the heat loss and increase SEUE. Although water is a good heat transfer fluid, adding nanomaterials into water can further improve its thermal conductivity. If Cu–H_2O nanofluids are used, the efficiency of FPSC can be improved by 24.52% (Zheng et al., 2015). Using Al_2O_3–water nanofluid as heat transfer fluid, the maximum energy efficiency of FPSC can be increased by 1% (Shojaeizadeh et al., 2015). SiO_2 nanofluids can save more than 280 MJ of embodied energy and offset 170 kg less CO_2 emissions (Faizal et al., 2015). Compared with nanofluids, such as SiO_2, CuO, Al_2O_3, and TiO_2, the efficiency of U-tube solar collector is the highest with 0.2 vol%-MWCNT nanofluid (Kim et al. 2016).

To sum up, the SEUE of FPSC can be more than 80% under experimental conditions by improving solar absorptance and reducing heat loss (Yandri 2019). However, the meteorological parameter and the operation mode will also have an impact on the SEUE of the collector system. In practice, the SEUE of solar hot water system is still very low, and the heat supply of the system does not even meet the design requirements. To improve the SEUE, based on the thermal performance of the existing collector, taking the meteorological parameters and the operation mode of the system as variables, this paper established the SEUE analysis model of the FPSC system. Through experimental tests and theoretical analysis, the influence of meteorological parameters and hot water system operating parameters on the SEUE of FPSC was studied. The research results can provide parameters basis for the design of solar hot water system. It provides a parameter basis for the design of FPSC system, especially the connection mode of collector and auxiliary heat device, and the design of system water temperature.

Analytical model

The principle of solar energy conversion and utilization of the collector is displayed in Fig. 1.

The total solar energy is I W/m^2 arriving the collector. Some of them are reflected by the collector, reflected and absorbed by the glass cover plate, or shielded by the collector frame. The energy loss rate is defined as μ. The heat energy absorbed by the collector is obtained as:

$$q_{abs} = I(1-\mu). \tag{1}$$

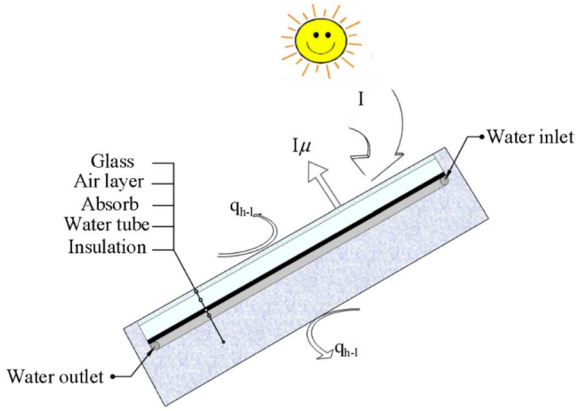

Fig. 1 Schematic of collector's working principle

Fig. 2 Experimental device

The heat loss of energy absorption process is obtained as:

$$q_{a-l} = I - q_{abs} = \mu I. \tag{2}$$

Solar energy is converted into heat energy by the collector. Some of the heat is absorbed to hot water for users, and the other part is lost to the external environment through the enclosure in the form of convection and radiation. The heat absorbed by hot water is obtained as:

$$q_w = cm(t_o - t_i). \tag{3}$$

The heat loss through the enclosure of the collector is defined as the heat loss of energy conversion process, which is obtained as:

$$q_{c-l} = U\left(\frac{t_i + t_o}{2} - t_a\right). \tag{4}$$

The total heat loss of the collector is the sum of heat loss of energy absorption process and energy conversion process, which is obtained as:

$$q_{t-l} = q_{o-l} + q_{h-l}. \tag{5}$$

The solar energy utilization efficiency (SEUE) was defined as the ratio of the heat transferred by the collector to the hot water and solar radiation intensity, which is obtained as:

$$\eta = \frac{q_w}{I} = 1 - \frac{q_{o-l} + q_{h-l}}{I} = 1 - \mu - \frac{U(\frac{t_i+t_o}{2} - t_a)}{I}. \tag{6}$$

From Eq. (6), it can be known that there are many factors affecting the SEUE of the collector, mainly including the absorption process loss, the heat transfer coefficient between the collector and the external environment, air temperature, the inlet water temperature, and outlet water temperature, solar radiation intensity, etc. In engineering design, to improve the SEUE, the collector material with a low loss rate for solar radiation and the structure with a small heat transfer coefficient between the collector and the surrounding environment are often selected. For the selected collector, the heat loss rate in the absorption process and heat transfer coefficient are unchanged. However, the solar radiation intensity and air temperature change hourly, and the supply and return water temperature may also change with seasons and user needs. From Eq. (6), the higher the water average temperature, or the lower the ambient temperature, will reduce the SEUE of the collector. Therefore, this paper will use the methods of experiment, analysis and calculation to further study the change law of these factors on the SEUE of the collector.

Experiment

Experimental device

As shown in Fig. 2, the experimental system was mainly composed of flat plate solar collector (FPSC), electric water heater, water pump, hot water tank, and so on. 10 FPSC 2000 mm × 1000 mm × 106 mm in size were used. The total collection area was 10m^2, and each collector was connected in parallel. The electric water heater heated water. Hot water at constant temperature was stored in a water tank and provided for the FPSC. The water pump was used to send the water from water tank to collectors. The water flow into the collector was set to 0.2 kg/s by using the flow regulating valve.

Table 1 Test instrument, type and parameter

Test parameters	Test instrument	Type	Accuracy
Solar radiation intensity	Solar pyrometer	TBQ-2	≤0.2%
Water flow	Ultrasonic flowmeter	TUF-JZ200SW	≤0.2%
Temperature	Thermal resistance	PT100	±0.2%
	Data acquisition unit	JK4000	≤0.3%

Experimental test methods

The experiment mainly measures the solar radiation intensity, air temperature, water flow value of collectors, outlet, and inlet water temperature of collectors. In the experimental test, PT-100 thermal resistance is used to measure the air temperature and water temperature. Temperature data were recorded by the data acquisition unit (JK4000). Solar irradiance was measured by radiation recorder (TBQ-2). An ultrasonic flowmeter (TUF-JZ200SW) was used to measure the water flow value. In the experiment, flow regulating valve was used to control water flow, and the inlet water temperature of collectors was determined by an electric heater and hot water tank. The test instruments and parameters are presented in Table 1.

Uncertainty analysis

In experiments, various errors cause the experimental results to deviate from the true value. The uncertainty analysis is the degree to which the measured value of the reaction is uncertain. According to the numerical evaluation method, it is usually divided into type A standard uncertainty and type B standard uncertainty. The type A standard uncertainty is evaluated by statistical methods. Type B standard uncertainty is evaluated by non-statistical methods and estimated by the previous experience or the assumed probability data distribution.

The calculation formula of type A standard uncertainty caused by limited repeated measurements is:

$$\sigma_A = \sqrt{\frac{\sum_{i=1}^{n} (x_i - \overline{x})^2}{n(n-1)}}. \tag{7}$$

The calculation formula of type B standard uncertainty caused by experimental instruments is:

$$\sigma_B = \frac{\alpha}{k}, \tag{8}$$

where α is the allowable error limit value for the instrument, and k is the confidence factor related to the confidence level.

The uncertainty of this experiment comes from relevant instruments and limited repeated measurements, and its calculation formula is:

$$\sigma = \sqrt{\sum_{i=1}^{n} \sigma_A^2 + \sigma_B^2}. \tag{9}$$

The calculation results of the experimental uncertainty are shown in Table 2.

Analysis of experimental results

The inlet flow value of the collector was 0.02 kg/(m^2·s). The experimental test of FPSC was carried out during the cold season in Hot Summer and Cold Winter Zones. Experimental results with good weather and different inlet water temperatures of the collector are selected, as shown in Fig. 3.

From Fig. 3, under the combined action of solar radiation intensity and air temperature, the SEUE and outlet water temperature gradually increase in the morning. With air temperature and solar irradiation decreasing gradually in the afternoon, outlet water temperature and SEUE decrease gradually. Solar irradiation displayed in Fig. 3 a reached the maximum value of 641 W/m^2 at 12:20. The air temperature increased from 6.8 °C at 7:00 to 15.2 °C at 13:50, and then gradually decreased to 10.0 °C at 20:00. When inlet water temperature was 17.9 °C, outlet water temperature increases gradually with the increase of solar radiation intensity and air temperature. In the morning, outlet water temperature increases gradually, from 17.4 °C to the maximum value of 22.3 °C. Then, it gradually decreased in the afternoon and decreased to 17.5 °C at 20:00. The change range of outlet water temperature was 4.9 °C. The SEUE changed greatly and its value was greater than 0% from 7:50 to 11:00. The solar irradiation and air temperature corresponding to the SEUE of 0% were 80 W/m^2 and 7.0 °C in the morning and 40 W/m^2 and 14.6 °C in the afternoon. From 9:10 to 16:40, the SEUE was greater than 50%, and the maximum value was 58%. Before 7:50 or after 17:10, the solar irradiation and air temperature were low, and the SEUE was negative. The solar irradiation dropped to 0 W/m^2 after 17:50, the air temperature

Table 2 The uncertainty of calculated values

Calculated values	Maximum uncertainty
Solar radiation intensity	*25 W/m^2*
Water flow	0.34m^3/h
Temperature	1.2 °C

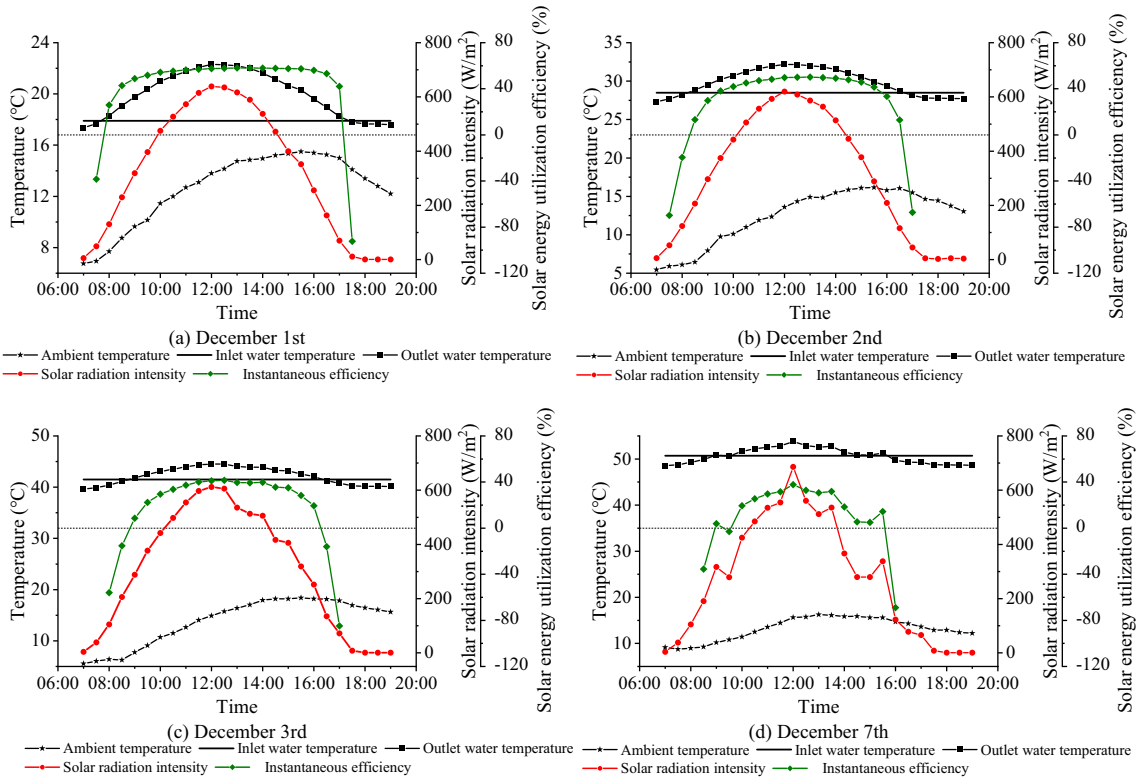

Fig. 3 Experimental test results

gradually decreases from 13.7 °C to 10.0 °C from 17:50 to 20:50, and the outlet water temperature of the collector decreases from 17.7 °C to 17.5 °C.

From 7:00 to 19:00, the maximum value of the solar radiation intensity in Fig. 3 b was 613 W/m^2. And air temperature went up from 5.5 °C to the maximum value of 16.3 °C at 14:50, and then gradually decreased to 13.1 °C. When the inlet water temperature was 2.85 °C, the outlet water temperature increases from 27.3 °C to the maximum value of 32.1 °C, and then gradually decreases to 27.7 °C, and the variation range of outlet water temperature was 4.8 °C. From 8:20 to 16:30, the SEUE of the collector was greater than 0%. When SEUE was 0%, the solar radiation intensity and air temperature were 124 W/m^2 and 6.1 °C in the morning and 116 W/m^2 and 16.1 °C in the afternoon. The maximum solar radiation intensity in Fig. 3 c was 612 W/m^2. The air temperature increased from 5.6 °C to 18.4 °C, reached a maximum value of 18.4 °C at 14:50, and then gradually decreased to 15.7 °C. When the inlet water temperature was 41.5 °C, the outlet water temperature gradually increased from 39.6 °C to the maximum value of 44.5 °C, and then gradually decreased to 40.1 °C. The change range of outlet water temperature was 4.9 °C. From 8:50 to 16:10, the SEUE is greater than 0%. When SEUE was 0%, the solar radiation intensity and air temperature were 262 W/m^2 and 7.5 °C in the morning and 200 W/m^2 and 18.3 °C in the afternoon. The maximum solar radiation intensity in Fig. 3 (c) was 686 W/m^2. The air temperature increased from 9.2 °C to 16.6 °C, reached a maximum value at 13:10, and then gradually decreased to 12.2 °C. When water inlet temperature was 50.7 °C, the water outlet temperature gradually increased from 48.5 °C to the maximum value of 53.8 °C, and then gradually decreased to 48.7 °C. The variation range of outlet water temperature was 5.3 °C. From 9:30 to 15:30, the SEUE is greater than 0%. When SEUE was 0%, the solar radiation intensity and air temperature were 317 W/m^2 and 10.2 °C in the morning and 262 W/m^2 and 16.2 °C in the afternoon.

Based on the above analysis, the changes in solar irradiation and air temperature will affect the SEUE and outlet water temperature of the collector. During the experimental time, the variation range of air temperature was 5.6 °C—18.4 °C. The variation range was 12.8 °C, and the variation range of solar radiation intensity was 0—686 W/m^2. The impact of solar irradiation on SEUE is greater than that of air temperature, because the change of air temperature is affected by the solar radiation intensity. In addition, inlet water temperature also has a significant impact on SEUE and outlet water temperature.

For the sake of further analyzing the thermal performance of the collector, according to the calculation method of the collector's normalization temperature, the difference between the average temperature of hot water and the air temperature is obtained. The normalization temperature is the ratio of the hourly temperature difference to the hourly solar irradiation, which is obtained as:

$$T^* = \frac{\frac{t_i + t_o}{2} - t_a}{I}. \tag{10}$$

According to the experimental data, the relationship between the normalization temperature and the SEUE was obtained, as shown in Fig. 4.

It can be observed from Fig. 4 that the SEUE varied linearly with the normalization temperature, and their fitting relationship was obtained as:

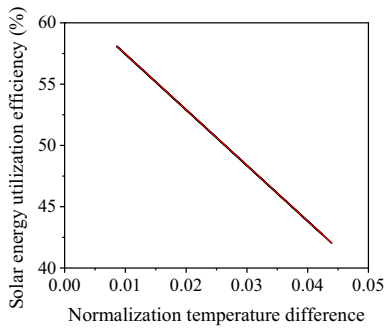

Fig. 4 Relationship between normalization temperature and solar energy utilization efficiency

$$\eta = 0.620 - 4.538T^*. \tag{11}$$

Equation 8 shows that even if the normalized temperature was 0, the SEUE of the collector is only 62%. There is no heat transfer between the collector and ambient, and heat loss of energy absorption process will also lead to a decrease in SEUE. Therefore, reducing the heat loss of energy absorption process and increasing the solar radiation absorption rate of the collector has an important impact on improving its SEUE.

Simulation results

The collector is connected in parallel with the auxiliary heat device

When the collector is connected in parallel with the auxiliary heating device, inlet and outlet water temperature of the collector is generally the supply and return water temperature of the system. The water flow of the collector was changed to maintain inlet and outlet water temperature when solar irradiation changed. The temperature difference between supply and return water was 10 °C. When inlet water temperature was 20, 30, 40, and 50 °C, the average water temperature of the collector was 25, 35, 45, and 55 °C, respectively. According to SEUE and the normalization temperature model, taking the meteorological parameters on December 1 as an example, the thermal performance is obtained for the collector, as shown in Fig. 5.

Figure 5 shows that the changing trend of heat loss, SEUE and water flow is similar to that of solar radiation intensity. The greater the solar irradiation, the more the heat loss of the collector. When air temperature

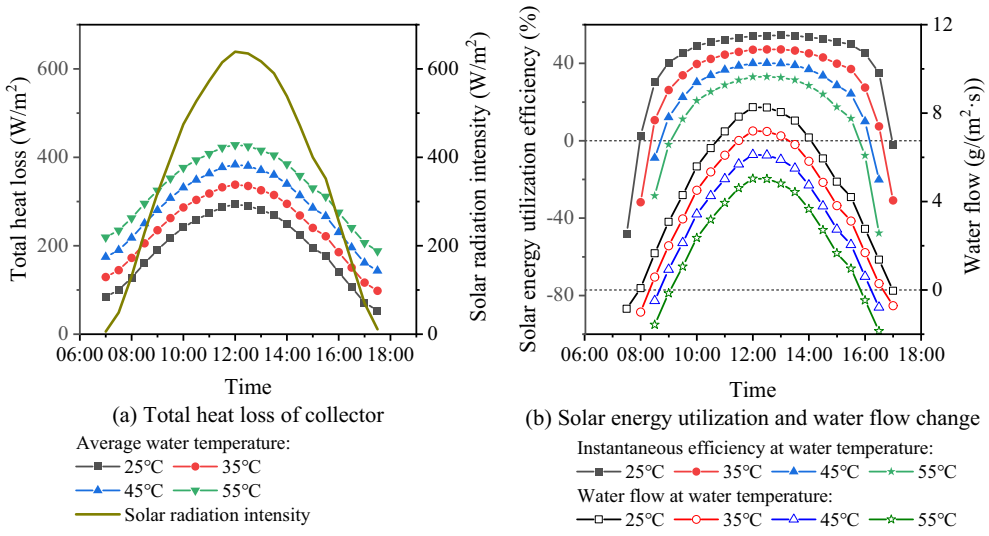

Fig. 5 The collector is connected in parallel with the auxiliary heat device

remained constant, the higher the water temperature, the greater the heat loss of the collector. At 7:00 am, when the solar irradiation was small, temperature difference between inlet and outlet water was maintained at a constant temperature of 10 °C. When the average water temperature was 25, 35, 45, and 55 °C, the heat loss of the collector was 84, 129, 174, and 219 W/m^2, respectively. The SEUE and water flow values were negative, and the heat loss was greater than solar radiation intensity. At this time, the collector did not provide heat for the system, becoming a heat dissipating device. In the morning, when SEUE is 0%, the water flow of the system is 0 g/(m^2·s). Under the four different temperature conditions, solar irradiation was 128, 193, 263, and 329 W/m^2, respectively. At this time, the collector could maintain temperature difference between supply and return water, but did not provide hot water for the system. At 12:20, solar irradiation reached the maximum value of 641 W/m^2. Under the four different temperature conditions, the heat loss of the collector was 292, 337, 382, and 427 W/m^2, respectively; the SEUE was 54.4%, 47.3%, 40.3%, and 33.3%, respectively; the water flow was 8.34, 7.26, 6.18, and 5.11 g/(m^2·s), respectively. This showed that the higher the hot water temperature, the greater the heat loss, the smaller the SEUE, and the smaller the water flow provided by the collector for the system.

From Fig. 5, each heat loss curve has two intersections with the solar radiation curve. Between the two intersections, solar irradiation was greater than the heat loss, and the collector could provide hot water for the system. Otherwise, water supply temperature of the collector cannot meet the system requirements. Among the four heat loss curves, the higher the hot water temperature, the shorter the distance between the two intersections of the heat loss curve and the solar radiation curve, indicating that the higher the hot water temperature, the shorter the time for the collector to provide hot water for the system normally. Under four different conditions, the heating time of the collector for the system was about 540 min, 500 min, 450 min and 390 min, respectively.

The collector is connected in series with the auxiliary heat device

The collector was connected in series with the auxiliary heat device, and water flow value was maintained constant. When solar irradiation changes, the inlet and outlet water temperature difference of the collector will be changed. The water flow was 20 g/(m^2·s). When the inlet water temperature was 20, 30, 40, and 50 °C, the change of thermal performance is shown in Fig. 6 for the collector.

From Fig. 6, at 7:00 am, the solar radiation intensity is very low, and water flow of the collector was maintained constant. When the average water temperature was 20, 30, 40 and 50 °C, heat loss was 60, 104, 148 and 192 W/m^2 for the collector, respectively. The solar irradiation was lower than heat loss, and the SEUE and water flow values were negative. At this time, the collector did not provide heat for the system, and became a heat dissipation device. In the morning, when SEUE is 0%, the water flow of the system is 0 g/(m^2·s). Under the four different temperature conditions, the solar irradiation was 99, 160, 227 and 296 W/m^2, respectively. At this time, the collector could maintain the temperature difference between supply and return water, but did not provide hot water for the system. The collector had normal water flow, but the

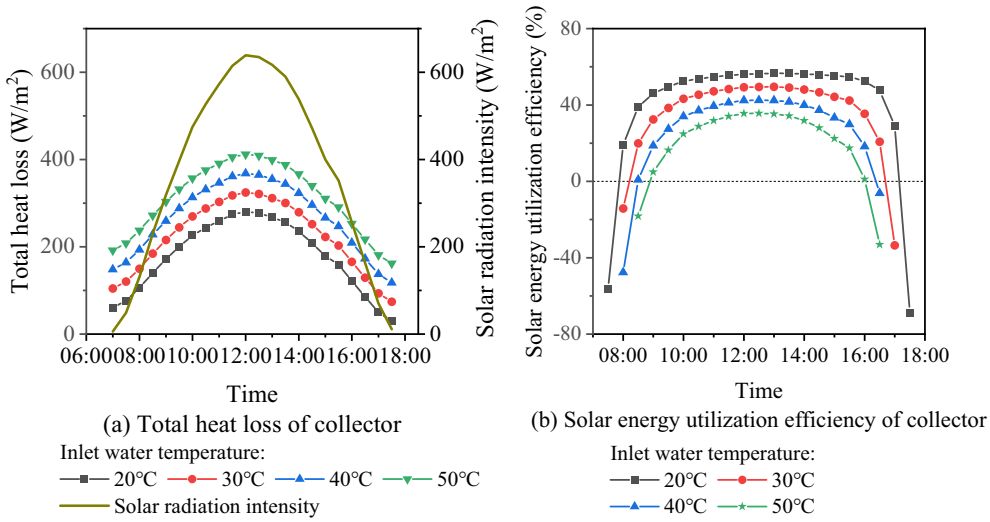

Fig. 6 The collector is connected in series with the auxiliary heating device

water inlet and outlet temperature were the same, which did not provide heat for the system. The maximum value of solar irradiation was 641 W/m^2. Under four different temperature conditions, the heat loss of the collector was 292, 337, 382 and 427 W/m^2, respectively and the SEUE was 54.4%, 47.3%, 40.3% and 33.3%, respectively. The higher the hot water temperature, the smaller the SEUE, the greater the heat loss of the collector, and the smaller the heat provided by the collector for the system. As also observed in Fig. 6, the intersection of each heat loss curve and solar radiation curve is similar to the parallel connection. Among the four heat loss curves, the higher the inlet water temperature, the shorter the distance between the two intersections of the heat loss curve and the solar radiation curve, showing that the shorter the timer to provide hot water for the system normally and the higher the hot water temperature. Under four conditions, the heating time for the collector was about 560, 520, 480 and 440 min, respectively.

In summary, with the same solar irradiation and air temperature, the series connection is a constant flow operation, the parallel connection is a constant temperature difference operation, and the average water temperature of the parallel connection is greater than that of the series connection. With the same water inlet temperature, the heat loss of the series connection is less than that of the parallel connection, and the SEUE of the series system is greater than that of the parallel. The main reason for the difference between parallel connection and series connection is that the average water temperature connected in parallel is higher than that in series.

Discussion and analysis

Changes in water temperature of the collector

Set the air temperature as 5 °C and the water flow of the collector as 20 g/(m^2·s) to analyze the impact of hot water temperature on SEUE. With solar irradiation as 100, 300, 500, 700, 900 and 1100 W/m^2, respectively, the relationship between water temperature and SEUE is shown in Fig. 7.

As observed in Fig. 7, the SEUE of the collector showed a linear correlation of water inlet temperature. When solar irradiation was constant, the lower the water inlet temperature the greater the SEUE. When the water inlet temperature was constant, the smaller the solar irradiation, the lower the SEUE. The smaller the solar irradiation, the greater the influence of inlet water temperature on SEUE. The solar irradiation was 100, 300, 500, 700, 900, and 1100 W/m^2, the inlet water temperature was 10 °C, SEUE was 38.5%, 53.1%, 56.0%, 57.2%, 57.9% and 58.4%, respectively. The higher the inlet water temperature, the greater the temperature difference between the collector and the air, resulting in greater heat loss and

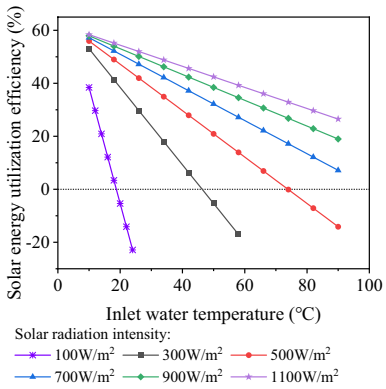

Fig. 7 Effect of inlet water temperature on solar energy utilization efficiency

smaller SEUE. As illustrated in Fig. 7, when SEUE was 0, the smaller the solar irradiation, the lower the water inlet temperature. When the solar irradiation was 100, 300 and 500 W/m^2, SEUE was 0%, the water inlet temperatures were 19, 46 and 74 °C, respectively. When the solar radiation intensity was greater than 700 W/m^2, even if the water inlet temperature was 90 °C, the SEUE was negative. Therefore, only if the inlet water temperature is less than the temperature corresponding to 0% SEUE, the collector could provide heat for the system normally. Otherwise, the SEUE will be negative, and the collector will become the heat dissipation device of the system.

The variation relationship between inlet water temperature and heat loss of collector is shown in Fig. 8.

As observed in Fig. 8, an increase in inlet water temperature led to an increase in total heat loss. When the inlet water temperature rose from 10 to 90 °C and the solar irradiation was 300, 500, 700 and 900 W/m^2, the heat loss increased from 141, 220, 299 and 379 W/m^2 to 491, 571, 650 and 729 W/m^2, respectively. The increase was about 350 W/m^2. When the inlet water temperature was 90 °C and solar irradiation was 300 W/m^2 or 500 W/m^2, the total heat loss of the collector was greater than the solar radiation intensity, and the collector could not provide heat for the system.

The total heat loss is the sum of heat loss of energy absorption process and conversion process. As illustrated in Fig. 8, when solar irradiation was unchanged, the heat loss of energy absorption process changed little with the change of water inlet temperature. The heat loss of energy absorption process was mainly caused by the transmittance of the glass cover, the solar absorptivity of the surface material, and the blocking of the solar rays by the collector's frame. For four solar radiation intensity, the heat loss of energy absorption process was about 114, 190, 266 and 342 W/m^2, respectively. The heat loss

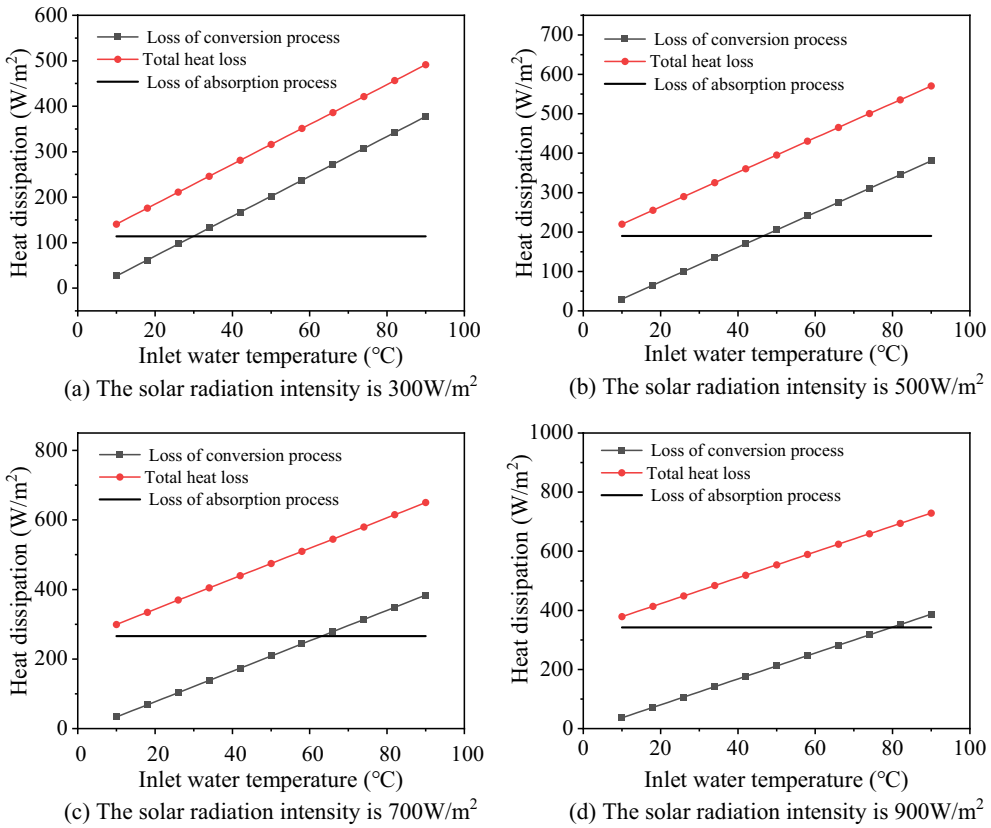

Fig. 8 Relationship between inlet water temperature and heat loss of collector

of energy conversion process increased with the increase of inlet water temperature. The heat loss of energy conversion process for the four solar radiation conditions were 27, 30, 33 and 37 W/m^2, respectively, when the inlet water temperature was 10 °C. The loss of conversion process was much less than that of absorption process. This is because the heat loss of energy conversion process is mainly due to the temperature difference between the collector and the air, and the temperature difference is very small. When the water inlet temperature rose to 90 °C, the heat loss of energy conversion process was 377, 381, 384 and 387 W/m^2, respectively. The increase of water temperature led to a great increase of heat loss in the conversion process. Under the four solar irradiation conditions, heat loss rate in the conversion process was 4.38 W/(m^2·°C). With the same inlet water temperature, the higher solar radiation intensity caused a greater heat collected by the collector, leading to a higher temperature difference between the absorber plate and the hot water. Therefore, even if the average water temperature of the collector is the same, the heat loss of energy conversion process will increase with the solar irradiation increased.

From Fig. 8, the smaller the solar irradiation, the greater the proportion of heat loss of energy conversion process in the total heat loss. When solar irradiation was 300 W/m^2, the inlet water temperature was greater than 30 °C, the heat loss of energy conversion process was greater than that of energy absorption process. When solar irradiation was 500, 700 and 900 W/m^2, the inlet water temperature was 46, 63 and 80 °C, respectively.

In summary, when solar irradiation was constant, reducing the inlet water temperature can improve SEUE. Therefore, the solar irradiation in winter is generally small in China's Hot Summer and Cold Winter Zones, the use of solar collectors for heating cannot meet the demand for building heat load, needing to set up auxiliary heat sources. If a combined heating system with FPSC and other auxiliary heat sources is used, the collectors and auxiliary heat sources are connected in series with collector priority, which has a higher SEUE than parallel connections. The need for cooling in summer and heating in winter in Hot Summer and Cold Winter Zones, and the general summer cooling load value is greater than the winter heat load. The chilled water

supply/return temperature for summer cooling is often 7/12 °C, and the indoor air temperature is controlled at 26 °C, so the heat exchange temperature difference between chilled water and indoor air is 16.5 °C. If the winter indoor heating temperature is controlled to 20 °C, using the same indoor air and hot water heat exchange temperature difference, the average temperature of hot water is 36.5 °C to meet the winter heating demand, and its value is lower than the existing hot water temperature for winter heating in Hot Summer and Cold Winter Zones. Therefore, lowering the hot water temperature can further increase the SEUE for the system while meeting the indoor thermal comfort conditions. Under low solar irradiation, the higher the water supply temperature of the collector, the easier it is to dissipate the heat of the system into the environment. Therefore, When the solar irradiation decreases until SEUE is 0%, the collector should stop running and prevent the hot water from entering the collector.

Changes in solar radiation intensity

Hot water flow of the collector was 20 g/(m^2·s), and air temperature was 5 °C. The influence of solar radiation intensity on SEUE is shown in Fig. 9.

As depicted in Fig. 9, the SEUE increased with the increase of solar irradiation. The greater the solar irradiation, the smaller the impact of the changes in solar irradiation on SEUE. When solar irradiation was small, SEUE was negative. When the water inlet temperature was 20, 30, 40, and 50 °C, the SEUE was 0%, the corresponding solar irradiation was 113, 184, 255, and 328 W/m^2, respectively. When solar irradiation was greater than the corresponding value, the SEUE was greater than 0%, to provide heat for the system. Otherwise, the collector may lose the heat of the system. The reason is that the air temperature is lower than the average temperature of the collector. If the water inlet and outlet temperature of the collector were constant, there will be the heat loss of energy conversion process between the collector and air, resulting in the heat obtained by the collector being less than heat loss. From Fig. 9, SEUE was small under the simulating conditions. When solar irradiation intensity was 300 W/m^2, the SEUE to water temperatures of 20, 30, 40 and 50 °C are 3.85%, 23.8%, 9.2% and -5.4%, respectively. Even when solar irradiation was 600 W/m^2, the SEUE was only 49.4%, 42.1%, 34.8% and 27.5%, respectively. With the average water temperature was different, the heat loss had a great impact on SEUE.

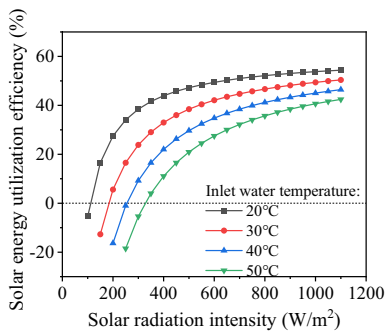

Fig. 9 Effect of solar radiation intensity on solar energy utilization efficiency

The relationship between the heat loss of the collector and the solar radiation intensity is displayed in Fig. 10.

As observed in Fig. 10, total heat loss of the collector increased with an increase of solar radiation intensity. When water inlet temperature of the collector was 20, 30, 40 and 50 °C, the solar irradiation rose from 50 to 1100 W/m^2, the total heat loss increased from 74, 117, 161 and 205 W/m^2 to 502, 546, 589 and 633 W/m^2, respectively. The increase of total heat loss was about 428 W/m^2. Under the four water inlet temperature conditions, when solar irradiation was weak, the total heat loss of the collector was greater than solar radiation intensity. In this situation, the collector cannot supply heat for the system. As illustrated in Fig. 10, when water temperature was constant, the heat loss of energy conversion process was caused by the changes of solar radiation intensity under that of energy absorption process. When solar irradiation was enhanced from 50 to 1100 W/m^2, the heat loss of energy conversion process increased from 66, 110, 154 and 198 W/m^2 to 84, 127, 171 and 215 W/m^2, respectively. The increase was about 17 W/m^2. The heat loss of energy absorption process increased from 8 to 418 W/m^2. And the variation range of the heat loss in the energy conversion process was much smaller than that in the energy absorption process. When solar irradiation was 180, 300, 425 and 550 W/m^2, under the four water temperature conditions, the heat loss of energy conversion process was equal to that of energy absorption process. And the heat loss of energy conversion process was 70, 114, 160 and 205 W/m^2, respectively. If the solar radiation continued to increase, the heat loss of energy absorption process will be greater than that of energy conversion process.

Based on the above analysis, under the simulation conditions, when the water temperature of the collector is constant, an increase of SEUE was caused by an increase of solar radiation intensity. However, the heat loss of the collector also rose with the enhancement of solar radiation intensity. With strong solar irradiation, the heat loss of energy absorption process is significantly greater than that of energy conversion process. Therefore, in addition to reducing the water temperature, promoting SEUE also

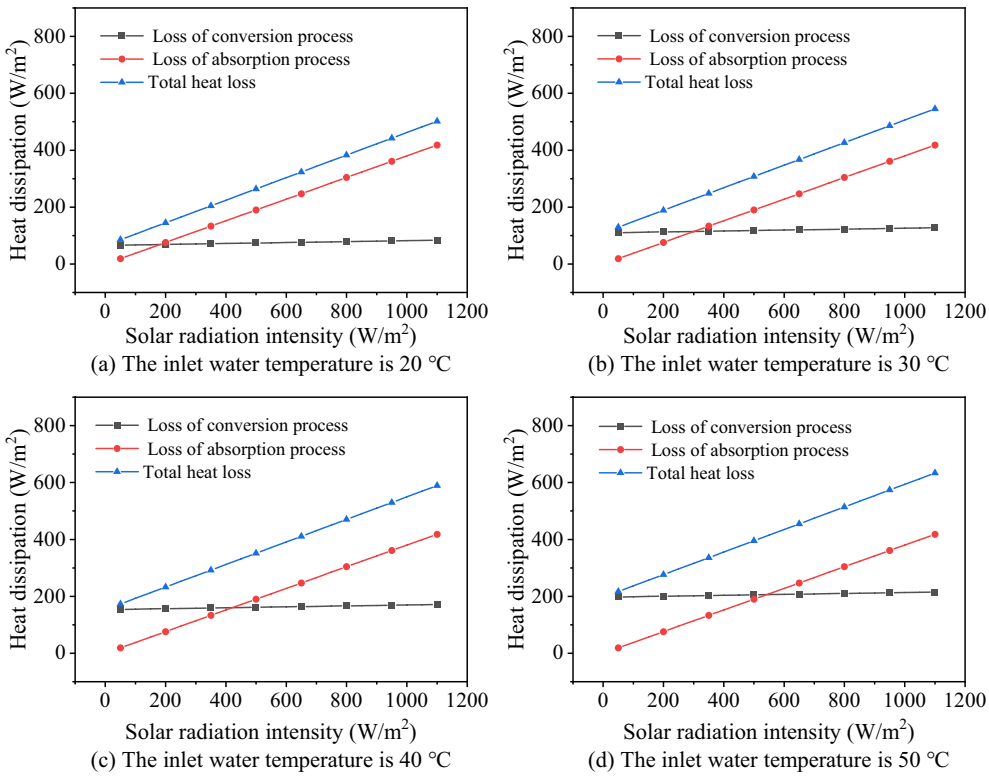

Fig. 10 Relationship between solar radiation intensity and heat loss of collector

can improve the thermal performance of the collector. If solar irradiation is weak, it can be considered to improve the absorptivity of the collector and reduce the heat loss to promote SEUE. When solar irradiation is strong, the effect of improving the absorptivity of the collector is more significant.

Operation optimization method

The SEUE of the collector is the key to affect the normal operation of solar water heating system. From the above research, in addition to the energy loss caused by the collector's material, structure and other factors, meteorological parameters such as solar radiation intensity and air temperature, and operating parameters such as the inlet and outlet water temperature will also affect the SEUE of the collector. To improve the SEUE, the supply and return water temperature of the collector can be reasonably adjusted according to the users' heating demand. For example, the temperature of domestic hot water in winter is generally above 50 ℃, and the heating temperature is related to the heating equipment used. The temperature of heating medium for floor heating, coil heating and radiator heating varies greatly. To improve the SEUE, you can choose appropriate user heating equipment to reduce the supply and return water temperature of the collector as much as possible.

In addition, in areas with low solar radiation intensity, the SEUE of the series connection mode of the collector and the auxiliary heat device is greater than that of the parallel connection. When supply and return water temperature of the system remains unchanged, the series connection mode is preferred, which can further reduce the average water temperature in the collector and improve SEUE. However, when the solar radiation intensity is very small or there is no solar radiation at night, the collector may become the heat dissipation equipment of the system. Under the simulated conditions, when the SEUE was 0%, the inlet water temperature of the collector was 20, 30, 40 and 50 ℃, respectively, and the corresponding solar radiation intensity was 128, 193, 263 and 329 W/m^2 for the parallel connection system and 99, 160, 227 and 296 W/m^2 for the series connection system. At this time, whether it is connected in parallel or series, when the solar radiation intensity is lower than the working condition with SEUE of 0%, the collector should be stopped, and the water inlet valve of the collector should be closed to prevent system heat loss through the collector.

Conclusion

This paper studied the SEUE of FPSC under different operating conditions. The relational model between SEUE and normalization temperature was established. The effects of the connection mode between the collector and the auxiliary heat source, water temperature and solar radiation intensity on SEUE were simulated and analyzed. The following conclusions were obtained:

1) The model for calculating SEUE of collector was established. The solar radiation intensity total heat loss rate of the collector, and air temperature are important parameters affecting SEUE. Solar irradiation has a great effect on SEUE.
2) The SEUE of the series connection system of collector and auxiliary heat device is greater than that of the parallel connection. When solar radiation intensity is weak, SEUE in parallel connection system reduce to 0% easily. In the simulation, when the water inlet temperature was 20, 30, 40 and 50 °C, SEUE was 0%, the corresponding solar radiation intensity of the parallel connection system was 128, 193, 263 and 329 W/m^2, respectively, and that of the series connection system was 99, 160, 227 and 296 W/m^2, respectively.
3) Reducing the inlet water temperature will lead to reducing the heat loss in the energy conversion process between the collector and the air and improve the SEUE. In the simulation, when the water inlet temperature was reduced from 50 °C to 30 °C, the SEUE increased from 38.5% to 48.2% with solar irradiation was 900 W/m^2. The SEUE can be improved by the hot water temperature of the collectors under the condition that the indoor heat load demand is met.

List of symbols

t_i: The collector inlet water temperature (°C); c: Specific heat capacity of water (J/(kg·K)); t_o: The collector outlet water temperature (°C); I: Solar radiation intensity (W/m^2); T^*: Normalized temperature difference; M: Mass flow of water in the collector (kg/s); U: Coefficient of heat loss per unit area W/(m^2·K); q_{abs}: Heat flux absorbed by the collector (W/m^2); μ: Loss rate of the collector to solar irradiation; $q_{a\text{-}i}$: Heat loss of energy absorption process (W/m^2); η: Solar energy utilization efficiency of the collector (%); $q_{c\text{-}i}$: Heat loss of energy conversion process (W/m^2); $q_{t\text{-}i}$: Total heat loss of the collector (W/m^2); q_w: Heat transfer from the collector to water (W/m^2); t_a: The air temperature (°C).

Abbreviations

FPSC: Flat plate solar collector; *SEUE*: Solar energy utilization efficiency.

Acknowledgements

Not applicable.

Author contributions

SX developed the key recommendation and wrote the main manuscript text. YZ analyzed the research status of the collector generating basis for the development of the recommendation. KX contributed to the design and construction of the experimental System and the test of experimental data. JL reviewed and revised the manuscript. All authors have reviewed and edited. All authors have read and agreed to the published version of the manuscript.

Funding

This work was supported by the Research Foundation of Education Bureau of Hunan Province (Grant Number: 20A499).

Availability of data and materials

All data generated or analyzed during this study are included in this published article.

Declarations

Ethical approval and consent to participate.

Not applicable.

Consent for publication

All the authors agree to publish the article.

Competing interests

The authors declare that they have no competing interests.

Author details

[1]China Aviation Changsha Design and Research CO.,LTD, Changsha 410000, China. [2]College of Civil Engineering, Xiangtan University, Xiangtan 411105, Hunan, China.

Received: 23 June 2022 Accepted: 29 August 2022
Published online: 17 September 2022

References

Ahmed, S. F., Khalid, M., Vaka, M., et al. (2021). Recent progress in solar water heaters and solar collectors: A comprehensive review[J]. *Thermal Science and Engineering Progress, 8*, 100981.

Balaji, K., Iniyan, S., & Goic, R. (2018). Thermal performance of solar water heater using velocity enhancer. *Renewable Energy, 115*, 887–895.

Colangelo, G., Favale, E., Miglietta, P., & de Risi, A. (2016). Innovation in flat solar thermal collectors: A review of the last ten years experimental results. *Renewable and Sustainable Energy Reviews, 57*, 1141–1159.

D'Alessandro, C., De Maio, D., Musto, M., De Luca, D., Di Gennaro, E., Bermel, P., & Russo, R. (2021). Performance analysis of evacuated solar thermal panels with an infrared mirror. *Performance Analysis of Evacuated Solar Thermal Panels with an Infrared Mirror, 288*, 116603.

Eaton, C. B., & Blu, H. A. (1975). The use of moderate vacuum environments as a means of increasing the collection efficiencies and operating temperatures of flat-plate solar collectors. *Solar Energy, 17*(3), 151–158.

Faizal, M., Saidur, R., Mekhilef, S., Hepbasli, A., & Mahbubul, I. M. (2015). Energy, economic, and environmental analysis of a flat-plate solar collector operated with SiO_2 nanofluid. *Clean Technologies & Environmental Policy, 17*, 1457.

Gao, D., Gao, G., Cao, J., Zhong, S., Ren, X., Dabwan, Y. N., & Pei, G. J. A. E. (2020). Experimental and numerical analysis of an efficiently optimized evacuated flat plate solar collector under medium temperature. *Applied Energy, 269*, 115129.

Gao, D., Zhong, S., Ren, X., et al. (2022). The energetic, exergetic, and mechanical comparison of two structurally optimized non-concentrating solar collectors for intermediate temperature applications[J]. *Renewable Energy, 184*, 881–898.

Giovannetti, F., FSte, S., Ehrmann, N., & Rockendorf, G. (2014). High transmittance, low emissivity glass covers for flat plate collectors: Applications and performance. *Solar Energy, 104*(104), 52–59.

Jamar, A., Majid, Z., Azmi, W., Norhafana, M., & Razak, A. (2016). A review of water heating system for solar energy applications. *International Communications in Heat and Mass Transfer, 76*, 178–187.

Jonas, D., Frey, G., & Theis, D. (2017). Simulation and performance analysis of combined parallel solar thermal and ground or air source heat pump systems. *Solar Energy, 150*, 500–511.

Joshi, D. N., Atchuta, S. R., Lokeswara Reddy, Y., Naveen Kumar, A., & Sakthivel, S. (2019). Superhydrophilic broadband anti-reflective coating with high weather stability for solar and optical applications. *Solar Energy Materials and Solar Cells, 200*, 110023.

Kim, H., Ham, J., Park, C., & Cho, H. (2016). Theoretical investigation of the efficiency of a U-tube solar collector using various nanofluids. *Energy, 94*, 497–507.

Liu, H., Tian, X., Ouyang, M., Wang, X., Dezhen, Wu., & Wang, X. (2021). Microencapsulating n-docosane phase change material into $CaCO_3/Fe_3O_4$ composites for high-efficient utilization of solar photothermal energy [J]. *Renewable Energy, 179*, 47–64.

The 13th Five-Year Plan for development of solar energy. National energy administration. http://zfxxgk.nea.gov.cn/auto87/201612/t20161216_2358.htm.

Qiu, Y., Xu, M., Li, Q., Xu, Y., & Wang, J. (2021). A novel evacuated receiver improved by a spectral-selective glass cover and rabbit-ear mirrors for parabolic trough collector - sciencedirect. *Energy Conversion and Management, 227*, 113589.

Seddaoui, A., Ramdane, M., & Noureddine, R. (2022). Performance investigation of a new designed vacuum flat plate solar water collector: A comparative theoretical study. *Solar Energy, 231*, 936–948.

Shojaeizadeh, E., Veysi, F., & Kamandi, A. (2015). Exergy efficiency investigation and optimization of an Al_2O_3-water nanofluid based Flat-plate solar collector. *Energy Build, 101*, 12–23.

Tahmineh, S., Alibakhsh, K., Kiana, R., Ameneh, H. H., Faezeh, A., & Omid, M. (2018). Thermoeconomic and environmental analysis of solar flat plate and evacuated tube collectors in cold climatic conditions. *Renewable Energy, 115*, 501–508.

Tschopp, D., Tian, Z., Berberich, M., Fan, J., Perers, B., & Furbo, S. (2020). Large-scale solar thermal systems in leading countries: A review and comparative study of Denmark, China. *Germany and Austria. Appl Energy, 270*, 114997. https://doi.org/10.1016/j.apenergy.2020.114997

U.S. Department of Energy, 2011 Buildings Energy Data Book, 2012.

Vesthmd, J., Roennelid, M., & Dalenbaeck, J. O. (2009). Thermal performance of gas-filled flat plate solar collectors[J]. *Solar Energy, 83*(6), 896–904.

Wang, D., Mo, Z., Liu, Y., et al. (2022). Thermal performance analysis of large-scale flat plate solar collectors and regional applicability in China. *Energy, 238*, 121931.

Wu, W., Wang, B., You, T., Shi, W., & Li, X. (2018). Configurations of solar air source absorption heat pump and comparisons with conventional solar heating. *Applied Thermal Engineering, 141*, 630–641.

Yandri, E. (2019). Development and experiment on the performance of polymeric hybrid photovoltaic thermal (PVT) collector with halogen solar simulator[J]. *Solar Energy Materials and Solar Cells, 201*, 110066.

Zhang, D., Tao, H., Wang, M., et al. (2017). Numerical simulation investigation on thermal performance of heat pipe flat-plate solar collector[J]. *Applied Thermal Engineering, 118*, 113–126.

Zheng, Z., He, Q., & Yin, S. (2015). Experimental investigation on efficiency of flat-plate solar collectors with Cu–H_2O nanofluids. *Taiyangneng Xuebao/acta Energiae Solaris Sinica, 36*(3), 562–567.

Publisher's Note